

**NASA
Technical
Paper
2468**

C.2
June 1985

**Exploratory Wind-Tunnel
Investigation of a
Wingtip-Mounted Vortex
Turbine for Vortex
Energy Recovery**

**James C. Patterson, Jr.,
and Stuart G. Flechner**

Property of U. S. Air Force
AEDC LIBRARY
F40600-81-C-0004

**TECHNICAL REPORTS
FILE COPY**

NASA

**NASA
Technical
Paper
2468**

1985

Exploratory Wind-Tunnel
Investigation of a
Wingtip-Mounted Vortex
Turbine for Vortex
Energy Recovery

James C. Patterson, Jr.,
and Stuart G. Flechner

*Langley Research Center
Hampton, Virginia*

NASA

National Aeronautics
and Space Administration

Scientific and Technical
Information Branch

Summary

An exploratory investigation has been conducted at the Langley Research Center to determine the possibility of recovering, with a turbine-type device, part of the energy loss associated with the lift-induced vortex system. Tests were conducted on a semi-span model with an unswept, untapered wing, with and without a wingtip-mounted vortex turbine. Three sets of turbine blades were tested to determine the effect of airfoil section shape and planform. The tests were conducted at a Mach number of 0.70 over an angle-of-attack range from 0° to 4° at a Reynolds number of 3.82×10^6 based on the wing reference chord of 13 in.

The data indicate that it is possible to recover rotational energy from the lift-induced vortex and obtain a reduction in induced drag with a four-bladed vortex turbine such as the one used in this investigation. The untapered turbine blades with a cambered airfoil section produced higher shaft power recovery than the untapered or tapered blades with symmetrical airfoil sections. The tapered blades produced a greater reduction in wing-induced drag than the untapered blades.

Introduction

The lift-induced vortex created by a three-dimensional wing under lifting conditions is a by-product of lift, and the effect of this vortex flow field on the downwash field just after the wing trailing edge results in an induced angle of attack that is responsible for the induced drag. This drag is equal to approximately 35 to 40 percent of the total cruise drag of a transport-type aircraft. An attempt has been made to recover a portion of this large energy loss by positioning a small turbine device in the center of the wingtip vortex to convert this vortical energy into usable rotational shaft energy and thereby minimize the energy extracted from the aircraft engines. With this device, part of the vortex can be relocated at the turbine blade tips. This relocation moves the vortex away from the wing in a manner similar to that of the winglet shown in reference 1 and reduces the induced drag of the aircraft. The turbine power generated by the vortex (extracted energy) could be employed to drive pumps or generators as part of a wing boundary layer control system or be utilized by the all-electric aircraft system.

To provide a preliminary indication of the effectiveness of the turbine in extracting rotational power from the vortex and in reducing induced drag, an exploratory wind-tunnel investigation has been conducted in the Langley 8-Foot Transonic Pressure Tunnel. The investigation was conducted on a semi-

span model with a vortex turbine mounted at the tip of an unswept, untapered wing having a symmetrical airfoil section. Tests were conducted with untapered turbine blades with both symmetrical and cambered airfoil sections and with tapered blades with symmetrical airfoil sections. All tests were conducted at a Mach number of 0.70, at angles of attack from approximately 0° to 4° , and at a Reynolds number of 3.82×10^6 based on a chord of 13 in.

Symbols

C_D	drag coefficient, $\frac{\text{Drag}}{qS}$
ΔC_D	change in drag coefficient measured from $\alpha = 0^\circ$
C_L	lift coefficient, $\frac{\text{Lift}}{qS}$
ΔC_L^2	change in C_L^2 measured from $\alpha = 0^\circ$
C_m	pitching-moment coefficient, $\frac{\text{Pitching moment}}{qSc_{\text{ref}}}$
C_P	power coefficient, $\frac{2\pi\eta r}{qSV_\infty}$
c_{ref}	wing reference chord, 13.0000 in.
c_t	turbine blade local chord
l_{bf}	length of balance fairing (fuselage), 126 in.
l_n	length of vortex turbine nacelle, 30.0 in.
l_{wf}	length of wing fairing, 30.8 in.
q	free-stream dynamic pressure, lb/ft ²
r	radius
S	exposed semispan reference area, 3.25 ft ²
V_R	resultant velocity
V_{vortex}	vortex velocity
V_∞	free-stream velocity, ft/sec
x	longitudinal distance measured from leading edge or nose
z	vertical distance measured from leading edge or nose
α	angle of attack, deg
η	rotational speed, revolutions per second
τ	turbine torque, ft-lb

Apparatus and Experimental Methods

Test Facility

This investigation was conducted in the Langley 8-Foot Transonic Pressure Tunnel, which is capable

of continuous operation through the subsonic, transonic, and low-supersonic speed ranges. The test section of the wind tunnel has a slotted floor and ceiling with solid walls, as shown in figure 1. The slots reduce the wall interference and allow tests of relatively large models at subsonic speeds. (See ref. 2.) The model used in the present investigation has a wing semispan equal to approximately 50 percent of the tunnel width and a fuselage, wing, and vortex turbine frontal area equal to approximately 2.6 percent of the cross-sectional area of the tunnel test section.

Model Configuration

A drawing of the semispan model used during the investigation is shown in figure 2. A photograph of the model with the vortex turbine mounted on the wingtip is shown in figure 3. Coordinates for each model component are given in table I.

Wing. The unswept, essentially untapered wing shown in figure 2 has a chord of 13 in. over most of the span, an NACA 64₁A012 airfoil section, and an aspect ratio of 6.39 based on the full span of 83 in. and the chord of 13 in. The exposed wing area is used as a reference area for data reduction. The semispan wing was constructed of steel and designed to accommodate the vortex turbine device at the wingtip.

Vortex turbine. The turbine consisted of a main shaft, turbine blades, and a streamlined nacelle attached to the wingtip. The leading edges of the four turbine blades were located 1.25 in. behind the wing trailing edge. The turbine centerline and blade chord plane were aligned laterally with the flight path and set at an incidence angle of -3° relative to the wing plane. This positioned the turbine blades near the center of the vortex, which is located above the wing trailing edge. This incidence angle also results in minimum turbine nacelle and blade frontal area when the wing is at an angle of attack of 3° (α at which data analysis was made). Three types of unswept turbine blades were tested. The first set was untapered and had a symmetrical airfoil section (untapered symmetrical blades). The second set was untapered and had a cambered airfoil section (untapered cambered blades). The third set was tapered and had symmetrical airfoil sections (tapered symmetrical blades). All three sets of turbine blades, shown in figure 4, were set at zero incidence relative to the turbine nacelle centerline.

Boundary layer transition strips, 0.125 in. wide, consisting of No. 120 carborundum grains, were installed on the upper and lower surfaces of the wing at

the 5.4-percent chord position and on the untapered symmetrical and cambered blades at the 5.5-percent chord position. This same size strip was also applied to the tapered blades, but its position varied linearly from 5.5 percent of the chord at the root to 3.5 percent of the chord at the tip.

Design philosophy. The vorticity shed from an aircraft is a function of the weight of the aircraft and is responsible for approximately 35 to 40 percent of the drag of transport-type aircraft. This vortex drag (induced drag) is a result of the additional downwash velocity behind the wing caused by the vortex flow and results in a reduction in the effective angle of attack of the wing. The largest effects stem from the region of the wingtip where the changes in the lift distribution are the greatest and the tip vortex is formed.

An example of the vortex flow created by a lifting wing ($\alpha = 6^\circ$) is shown in the flow visualization photograph presented in figure 5. The semispan wing, shown in the photograph, is being propelled along a track toward the viewer in the Langley Vortex Research Facility at 100 ft/sec. The lift-induced vortex is made visible by the use of smoke (ref. 3) and is seen just to the right of the wingtip.

It was proposed that it might be possible to recover part of this wasted energy, which must be supplied by the aircraft propulsion system, without significant effect on the airplane total drag. A turbine was designed to be mounted on the wingtip and to be driven by the vortex flow. The rotational velocity of the tip vortex, in combination with the stream velocity, induces an angle of attack on the turbine blades in addition to that due to camber and twist (fig. 6). The resulting normal force causes the blades to rotate in the direction shown. If the blades are extracting power from the vortex, the rotational speed of the generator will be below autorotation. Under this circumstance there will be an induced drag contributed by the wake of each blade. This blade-induced drag is offset by the reduction in wing-induced drag. When the blades are under load, there is a reduction in the rotational energy of the wingtip vortex, which is the main cause of wing-induced drag.

Since the blades are lifting, they will shed a small vortex from both the blade tip and root. The relative strength of the root and tip vortices will depend on the velocity distribution in, and magnitude of, the wingtip vortex, as well as the geometry, camber, and incidence distribution of the generator turbine blades. It can be postulated that the vortices from the roots of the blades, which all have the same direction of rotation (i.e., opposite to the blade tip vortices) will interact with each other and attenuate

more rapidly than the blade tip vortices. This could have a beneficial effect on wing-induced drag beyond that obtained by the antiswirl effect of the blades under load. Another possibility is that the load distribution on the blades is such that only weak vortices emanate from the root juncture. This is believed to be possible because the "end plate" effect of the turbine hub gives rise to a load distribution that is rather flat near the hub. The effect of the blade tip vortices on the induced drag of the wing may also be reduced because of their position with respect to each other and their direction of rotation.

Instrumentation

Force balance. Measurements of forces and moments were obtained from an internally mounted, wall-supported, five-component electrical strain-gauge balance. The model was designed so that the wing attached directly to the balance and protruded through a clearance opening in the fuselage, which was nonmetric. The fuselage (actually a balance fairing) was attached to the balance wall-support system but not to the balance. This arrangement allowed the fuselage to traverse through the angle-of-attack range without the fuselage forces being measured by the balance.

Vortex turbine power measurements. To determine the power absorbed by the vortex turbine, it was necessary to determine the torque developed by the turbine as well as its rotational speed. Because of the small size of the turbine nacelle, the usual method of coupling an electric generator to the turbine shaft was not possible. Hence, it was necessary to transmit the turbine torque by a shaft installed inside the removable leading edge of the wing, which was connected through a set of 90° bevel gears to the turbine shaft at the wingtip and to an electrical clutch located just inside the fuselage. This clutch was mounted on the metric side of the balance and was used as a prony brake to measure turbine torque. The torque required to reduce the rotational speed of the turbine below the maximum turbine speed (no-load condition) is related to the electrical current by calibration. The measured torque values developed by the turbine include any frictional losses due to the gears and shaft bearings and are therefore conservative for these tests. The turbine rotational speed was measured by a magnetic pickup located inside the turbine nacelle.

Tests. The wall-mounted semispan model used in this investigation is shown in the Langley 8-Foot Transonic Pressure Tunnel in figure 3, with the

wingtip-mounted vortex turbine. Tests were conducted at a Mach number of 0.70 over an angle-of-attack range from 0° to 4° at a total pressure of 2120 lb/ft² and a total temperature of 120°F. These conditions resulted in a Reynolds number of 3.82×10^6 based on the reference chord of 13 in.

The wing-fuselage was tested as a baseline configuration with a symmetrical fairing (based on the wing coordinates) installed on the wingtip. The turbine blades were tested in the static (nonrotating) mode of operation shown in figure 3. The turbine blades produce their maximum force in the nonrotating mode because the relative angle of attack (vortex flow/turbine blade) is at a maximum. In this position, the greatest reduction in induced drag is achieved.

The rotational speed used to determine the effectiveness of the vortex turbine was arbitrarily chosen to be one-half the maximum rotational speed attained by the turbine configuration in the free wheel (no-load) condition at each angle of attack. (Subsequent analysis has shown that this rotational speed produces very nearly maximum power.) The turbine was tested with each of the three different sets of turbine blades shown in figure 4. The turbine was set at an incidence angle of -3° relative to the wing chord to center the blades in the vortex and so that the turbine would be at zero angle of attack when the wing was at $\alpha = 3^\circ$ the approximate angle of attack at which the data analysis was to be made.

Each set of turbine blades was mounted at zero incidence relative to the centerline of the turbine body for low-drag considerations and to assure that the vortex turbine was affected by the vortex flow only.

Accuracy. Based on balance calibrations and repeatability, the accuracy of the data is estimated to be within the following limits:

C_L	±0.01
C_D	±0.0003
α , deg	±0.05
C_m	±0.001
Torque, ft-lb	±0.05

Results and Discussion

Presentation of Results

The results of this investigation are plotted in the following figures:

Vortex turbine energy recovery	Figure 7
Drag coefficient versus lift coefficient:	

Effect of turbine with untapered and tapered symmetrical blades	8(a)
Effect of turbine with untapered cambered blades	8(b)
Lift coefficient versus angle of attack and pitching-moment coefficient:	
Effect of turbine with untapered and tapered symmetrical blades	9(a)
Effect of turbine with untapered cambered blades	9(b)
Drag-due-to-lift factor	10

Vortex Relative Velocity

A vortex turbine, designed to recover part of the vortex-induced energy loss, may be installed at the wingtip in a manner similar to that shown in figure 6. The relative velocity vector (V_R), shown in this figure for the top blade only, is the vector sum of the free-stream velocity and the vortex velocity, which is approximately perpendicular to the flight path. The angle of V_R relative to the vortex turbine blades is responsible for the normal force generated by the turbine blades and causes them to rotate in the direction shown.

When the normal force produced by each turbine blade is resolved into lift, there is a thrust due to lift which is comparable to the reduction in induced drag caused by the vortex turbine.

Vortex Energy Recovery

The power recovered from the vortex by the three turbine blade designs is presented in figure 7 as the power coefficient, C_P , over the angle-of-attack range investigated. The power results, which are a consequence of the torque developed by the vortex turbine and its rotational speed, indicate that the power recovery of the turbine with untapered cambered blades is approximately three times that of the turbine with untapered symmetrical blades at a wing angle-of-attack of 3° . Turbine blade camber would be expected to produce more lift at the same blade angle of attack and therefore to generate more power. The results for the turbine with tapered symmetrical blades are approximately the same as those for the turbine with untapered symmetrical blades. These results may indicate that the outer area of the untapered symmetrical blade is not beneficial in producing torque and could be removed to eliminate the associated blade drag.

The effect of taper on turbine blades having symmetrical airfoil sections may also apply to cambered blades. Tapering cambered turbine blades would result in lower wing-induced drag, lower blade drag, and lower blade weight while possibly obtaining the

favorable effect of blade camber. Blade twist may also improve the turbine performance of each type of blade.

These model test results, when scaled to a present-day wide-body transport aircraft at cruise altitude, indicate the possibility of obtaining approximately 400 horsepower from each wingtip. The power required for an aircraft using all-electric aircraft systems or that required for wing boundary layer control would be approximately equal to one-half the energy recovered by the vortex turbine having four untapered cambered blades.

Aerodynamic Effect of Vortex Turbine Blades

The aerodynamic effect of the addition of the vortex turbine having untapered or tapered symmetrical blades to the basic wing configuration is shown as a variation in drag coefficient with lift coefficient in figure 8(a). Data are presented for the turbine in the static mode and at the blade rotation speeds noted at the data points. At zero lift there is an increase in the drag coefficient associated with the installation of the vortex turbine compared with the basic wing because of the additional wetted area of the turbine and its skin friction plus turbine form drag. At zero lift coefficient no vortex exists; therefore, there is no turbine rotation because the symmetrical turbine blades are affected only by the vortex flow. As the lift coefficient of the wing is increased, the turbine begins to rotate under the influence of the lift-induced vortex flow. The maximum tangential vortex velocity of the fully developed vortex is approximately 30 percent of the stream velocity. When combined with this stream velocity, the vortex velocity produces a flow angle relative to the turbine blades (angle of attack) of approximately 15° (ref. 4). As the vortex turbine rotates, it provides usable rotational energy, which is accompanied by a small increase in induced drag (relative to the nonrotating turbine) resulting from the lower blade lift due to the lower blade angle of attack associated with turbine rotation. The turbine blades are then less able to turn the vortex flow; therefore, their attenuating effectiveness is reduced.

The increase in drag level associated with the addition of the vortex turbine to the wingtip at zero lift coefficient is no longer present at the wing lift coefficient of approximately 0.35 for the untapered symmetrical turbine blades. This change in induced drag results from the effect of the vortex turbine blade downwash on the vortex flow field. As the wing lift coefficient is increased further, the drag coefficient of the turbine configuration is even less than that of the basic wing. The lower drag for the turbine configuration results from an increase in effectiveness of the turbine with the increase in

turbine lift associated with the stronger vorticity shed by the wing. The strength of the vorticity shed by the wing is a direct function of weight or lift.

Aerodynamic Effect of Blade Taper

Taper was added to the turbine blades, as stated earlier, in an attempt to remove the part of the blade area, along with its associated drag, that is in the lower velocity circulatory region of the vortex that exists radially beyond the vortex core. The tapered turbine blades showed a larger reduction in wing-induced drag than the untapered blades having the same symmetrical airfoil sections. The tapered blades averaged approximately 20 drag counts less than the untapered blades between $C_L = 0.2$ and $C_L = 0.4$. (See fig. 8(a).) This reduction could possibly result from the fact that the center of lift of the tapered turbine blade is farther inboard. Thus, more vorticity is shed near the hub and therefore is dissipated, as suggested earlier.

Aerodynamic Effect of Blade Camber

To increase the rotational energy output of the vortex turbine, a cambered airfoil section was selected for the untapered turbine blade. The effect on the drag of the wing is presented in figure 8(b). The drag of the untapered cambered turbine blades is greater at zero lift than that of the untapered symmetrical turbine blades. (Compare figs. 8(a) and 8(b).) As the lift coefficient increases, a larger reduction in induced drag is obtained by the cambered blades, compared with the symmetrical blades. This may possibly be associated with the larger energy recovery (larger reduction in vortex strength) due to the cambered blades. The energy extracted from the vortex by the cambered blades is equal to approximately three times that extracted by the symmetrical turbine blades.

Vortex Alleviation

The change in the drag-due-to-lift factor resulting from the addition of each vortex turbine configuration to the basic wing is shown in figure 10. There is an increase in efficiency (decrease in $\Delta C_D / \Delta C_L^2$) associated with each blade design relative to the basic wing. The untapered cambered blades are twice as effective as the untapered symmetrical blades; again this effect may be the result of the greater energy recovery obtained by camber.

The energy recovery of the tapered symmetrical turbine blades, was approximately the same as that of the untapered symmetrical blades (fig. 7); but the drag-due-to-lift factor of the tapered symmetrical blades is even lower than that of the untapered

cambered blades (fig. 10). It is conjecture that the effect of the tapered-planform blades on the induced drag of the wing is possibly a result of the high blade loading near the turbine root, as stated earlier, where a larger part of the vorticity is shed, compared with the untapered blades, and is possibly dissipated by the turbine shaft and each of the opposing blade root vortices.

Pitching Moment

The increase in pitching moment at zero lift associated with the installation of the vortex turbine (see fig. 9) is possibly a result of the incidence angle of -3° of the turbine relative to the chord plane of the wing and of the position of the turbine blades behind the wing trailing edge. This moment is reduced as the lift coefficient of the wing and that of the turbine is increased with the increase in angle of attack of the wing. This increase in lift of the turbine blades is the result not only of a physical change in angle of attack, but also possibly of the aerodynamic change due to the vortex flow of the wing now being generated (upward flow on the blades outboard of the wingtip). As a result, the effect of the vortex turbine on pitching moment is zero at a lift coefficient of approximately 0.2 ($\alpha = 2^\circ$) rather than at the lift coefficient for $\alpha = 3^\circ$.

The untapered symmetrical, tapered symmetrical, and untapered cambered blades give similar pitch characteristics. The untapered symmetrical and cambered blades in the nonrotating mode have lower pitching-moment values over the lift range than those in the rotating mode. This could be attributed to the fact that only two of the four turbine blades are effective in the vertical direction in this mode of operation.

Concluding Remarks

An exploratory investigation has been conducted to determine the possibility of recovering part of the energy loss associated with the lift-induced vortex system with a wingtip-mounted vortex turbine. Three different types of turbine blades were tested—untapered blades with a symmetrical airfoil section, tapered blades with symmetrical airfoil sections, and untapered blades with a cambered airfoil section.

It has been shown experimentally that it is possible to recover part of the lift-induced vortex energy with a wingtip-mounted turbine device. This energy recovery is in the form of turbine rotational energy due to the cross flow provided by the vortex at the wingtip plus a reduction in induced drag of the wing. These data indicate that the rotational energy recovered by the untapered cambered turbine

blades is equal to approximately three times that recovered by the untapered or tapered symmetrical turbine blades. The tapered symmetrical turbine blades showed a larger reduction in wing-induced drag (approximately 20 counts lower between $C_L = 0.2$ and $C_L = 0.4$, than the untapered symmetrical turbine blades.

Improvement in the vortex turbine performance may possibly be obtained through turbine blade design. The most obvious change is the addition of cambered airfoil sections to the tapered blades. An increase in the number of turbine blades, a change in blade loading by varying the blade twist distribution, and the use of a more conventional turbine blade camber are other factors which could have a favorable effect on the vortex turbine performance.

NASA Langley Research Center
Hampton, VA 23665
May 21, 1985

References

1. Whitcomb, Richard T.: *A Design Approach and Selected Wind-Tunnel Results at High Subsonic Speeds for Wing-Tip Mounted Winglets*. NASA TN D-8260, 1976.
2. Wright, Ray H.; Ritchie, Virgil S.; and Pearson, Albin O.: *Characteristics of the Langley 8-Foot Transonic Tunnel With Slotted Test Section*. NACA Rep. 1389, 1958. (Supersedes NACA RM L51H10 by Wright and Ritchie and NACA RM L51K14 by Ritchie and Pearson.)
3. Patterson, James C., Jr.; and Jordan, Frank L., Jr.: *A Static-Air Flow Visualization Method To Obtain a Time History of the Lift-Induced Vortex and Circulation*. NASA TM X-72769, 1975.
4. Patterson, James C., Jr.: Vortex Attenuation Obtained in the Langley Vortex Research Facility. *J. Aircr.*, vol. 12, no. 9, Sept. 1975, pp. 745-749.

TABLE I. COORDINATES OF MODEL COMPONENTS

(a) Vortex turbine nacelle

$\frac{x}{l_n}$	$\frac{r}{l_n}$
0	0
.0018	.0044
.0088	.0098
.0140	.0132
.0211	.0168
.0316	.0211
.5265	.0263
.0702	.0306
.0877	.0329
.1053	.0342
.1228	.0350
.1316	.0351
.1404	.0351
.1579	.0351
.7368	.0351
.7509	.0351
.7684	.0374
.7860	.0341
.7895	.0398
.8211	.0316
.8386	.0298
.8561	.0277
.8912	.0254
.9088	.0229
.9263	.0200
.9439	.0172
.9561	.0099
.9789	.0053
1.0000	.0002

(b) Turbine blade with symmetrical airfoil

$\frac{x}{c_t}$	$\frac{z}{c_t}$
0	0
.0020	.00704
.0050	.01164
.0125	.01875
.0250	.02587
.0375	.03077
.0500	.03463
.0749	.04067
.1999	.04539
.1249	.04925
.1499	.05246
.1739	.05523
.1998	.05755
.2498	.06105
.2998	.06321
.3497	.06432
.3997	.06453
.4496	.06394
.4996	.06222
.5495	.05914
.5745	.05709
.5995	.05488
.6245	.05185
.6495	.04890
.6744	.04553
.6994	.04206
.7244	.03837
.7494	.03453
.7744	.03060
.7993	.02664
.8243	.02272
.8493	.01887
.8743	.01526
.8993	.01191
.9242	.00832
.9492	.00628
.9742	.00437
.9920	.00289
1.0000	.00284

TABLE I. Continued

(c) Turbine blade with cambered airfoil

$\frac{x}{c_t}$	$\left(\frac{z}{c_t}\right)_{\text{upper}}$	$\left(\frac{z}{c_t}\right)_{\text{lower}}$
0	0.00099	0.00099
.002	.00948	-.00627
.005	.01512	-.01525
.0125	.02429	-.02059
.025	.03445	-.02059
.0375	.04187	-.02440
.05	.04743	-.02745
.075	.05517	-.03228
.10	.06061	-.03608
.125	.06481	-.03920
.15	.06819	-.04182
.175	.07096	-.04400
.20	.07327	-.04581
.225	.07520	-.04728
.25	.07678	-.04847
.275	.07803	-.04941
.30	.07899	-.05013
.325	.07968	-.05065
.35	.08012	-.05096
.375	.08032	-.05106
.40	.08029	-.05092
.425	.08003	-.05051
.45	.07952	-.04981
.475	.07876	-.04881
.50	.07775	-.04751
.525	.07646	-.04592
.55	.07487	-.04402
.575	.07293	-.04181
.60	.07064	-.03927
.625	.06796	-.03643
.65	.06490	-.03001
.70	.05775	-.02657
.725	.05371	-.02307
.75	.04942	-.01957
.775	.04490	-.01614
.80	.04018	-.01288
.825	.03529	-.00990
.85	.03026	-.00729
.875	.02518	-.00514
.90	.02008	-.00354
.925	.01495	-.00261
.95	.00982	-.00252
.975	.00470	-.00354
1.000	-.00047	-.00605

(d) Wing with NACA 64₁A012 airfoil

$\frac{x}{c_{\text{ref}}}$	$\frac{z}{c_{\text{ref}}}$
0	0
.005	.00961
.0075	.01158
.0125	.01464
.025	.02018
.050	.02788
.075	.03364
.10	.03839
.15	.04580
.20	.05132
.25	.05534
.30	.05809
.35	.05965
.40	.05993
.45	.05863
.50	.05605
.55	.05244
.60	.04801
.65	.04289
.70	.03721
.75	.03118
.80	.02500
.85	.01882
.90	.01263
.95	.00644
1.00	.00025

TABLE I. Concluded

(e) Balance fairing

$\frac{x}{l_{bf}}$	$\frac{r}{l_{bf}}$
0	0
.004	.014
.008	.020
.012	.024
.016	.028
.020	.031
.024	.034
.028	.036
.032	.039
.063	.051
.079	.055
.095	.058
.111	.060
.127	.061
.143	.062
.659	.062
.683	.061
.702	.061
.722	.060
.742	.058
.762	.056
.782	.053
.802	.050
.821	.047
.842	.043
.881	.034
1.000	.005

(f) Wing fairing

$\frac{x}{l_{wf}}$	$\frac{r}{l_{wf}}$
0	0
.0065	.0195
.0097	.0227
.0162	.0292
.0227	.0347
.0292	.0390
.0389	.0438
.0584	.0519
.0649	.0545
.0811	.0597
.0973	.0642
.1140	.0681
.1290	.0701
.1460	.0720
.1780	.0743
.1950	.0746
.2110	.0753
.2270	.0753
.5510	.0753
.5840	.0753
.6160	.0720
.6490	.0691
.6910	.0655
.7140	.0615
.7460	.0568
.7780	.0509
.8110	.0454
.8430	.0396
.876	.0337
.9080	.0259
.9410	.0178
.9730	.0081
1.0	0

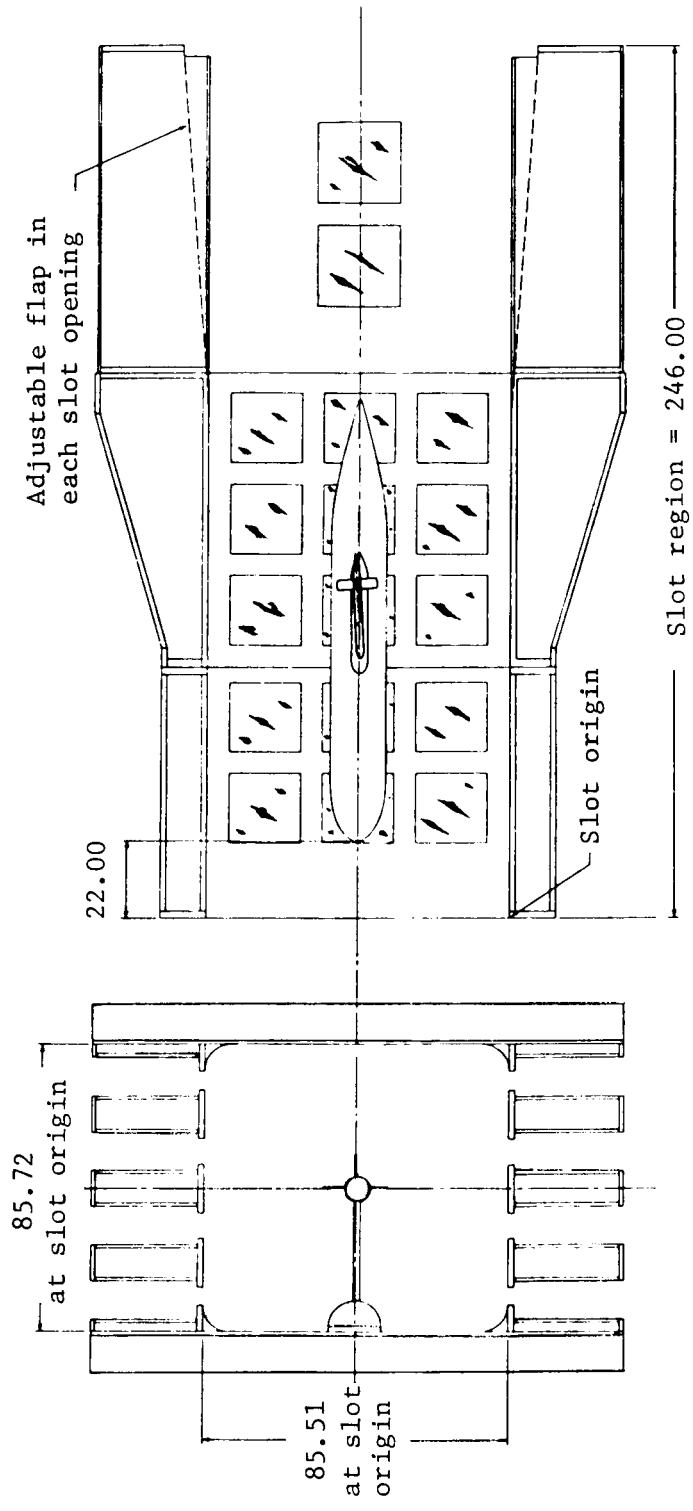


Figure 1. Model located in Langley 8-Foot Transonic Pressure Tunnel. All dimensions are in inches.

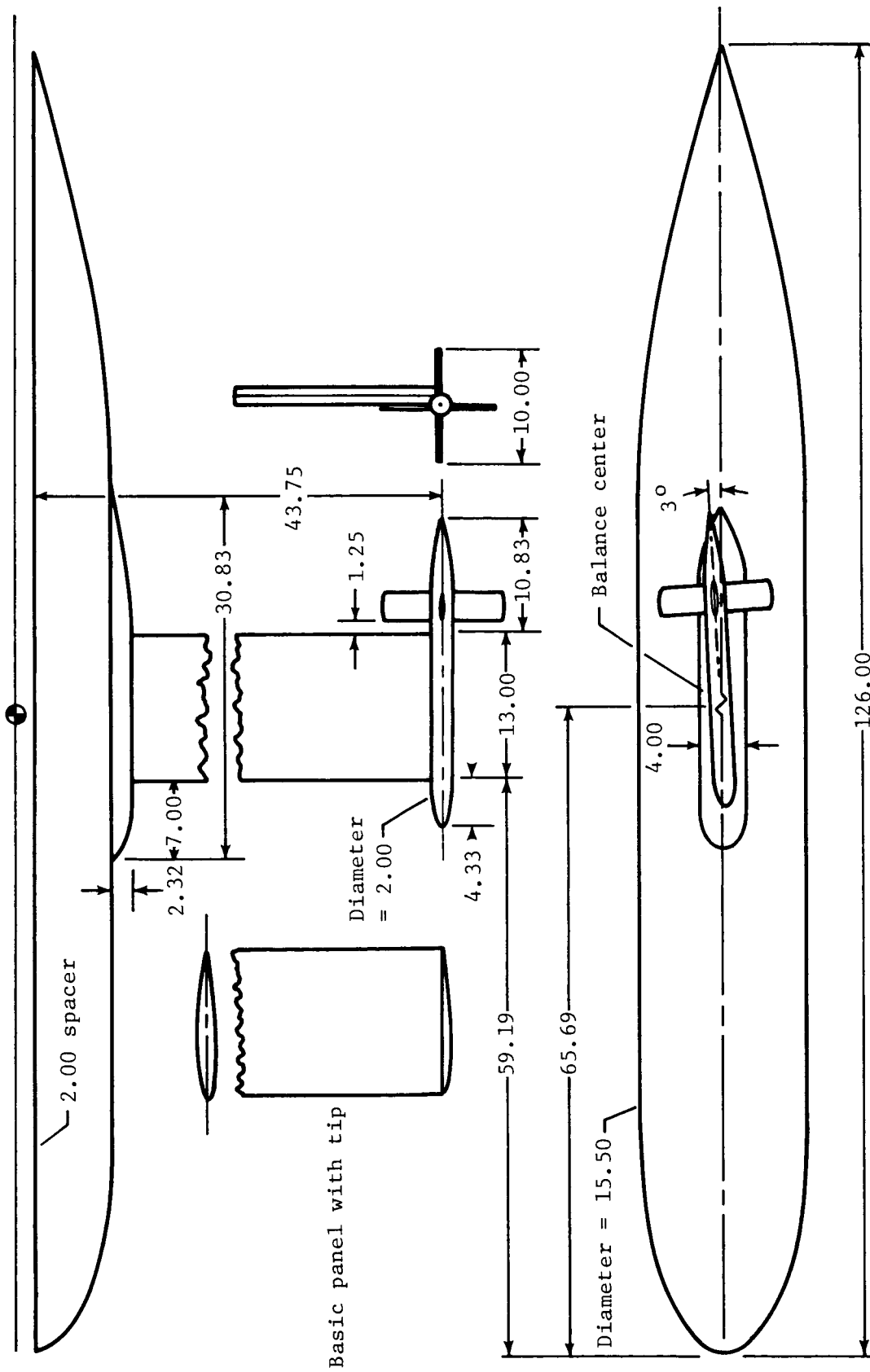
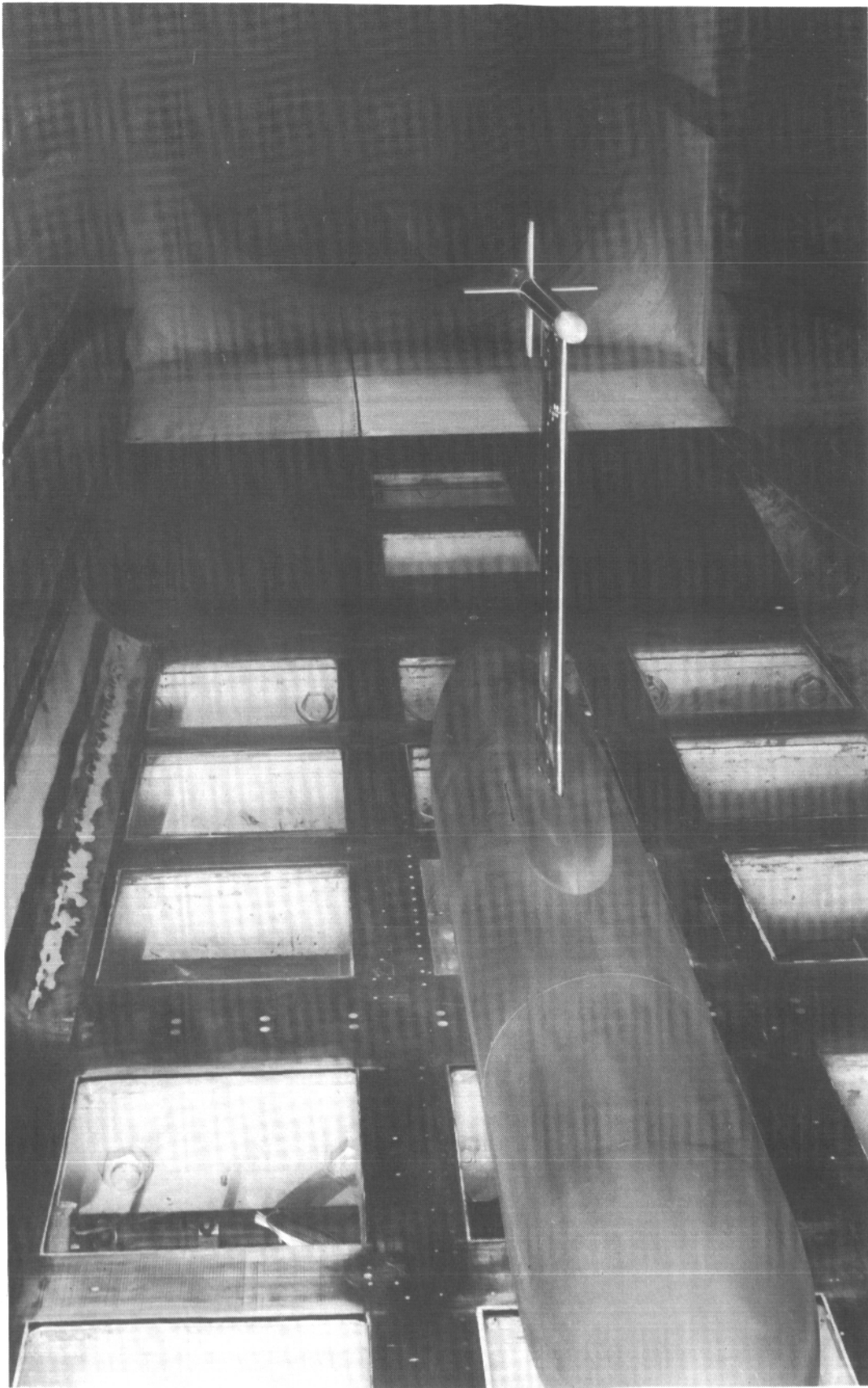


Figure 2. Drawing of semispan wind-tunnel model with wingtip-mounted vortex turbine. Dimensions are in inches unless otherwise noted.



L-81-5520

Figure 3. Photograph of wall-mounted semispan model in Langley 8-Foot Transonic Pressure Tunnel with vortex turbine on wingtip.

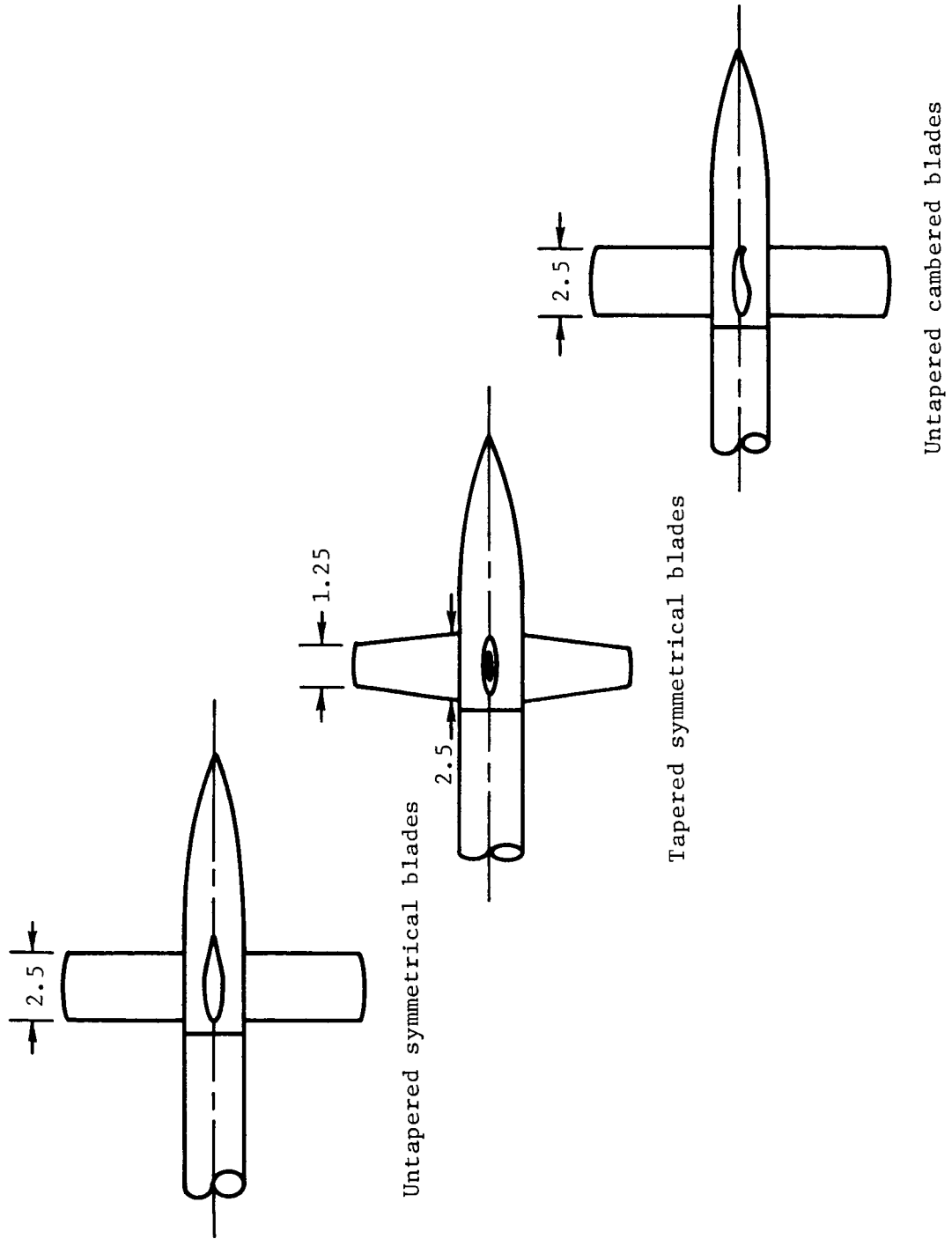
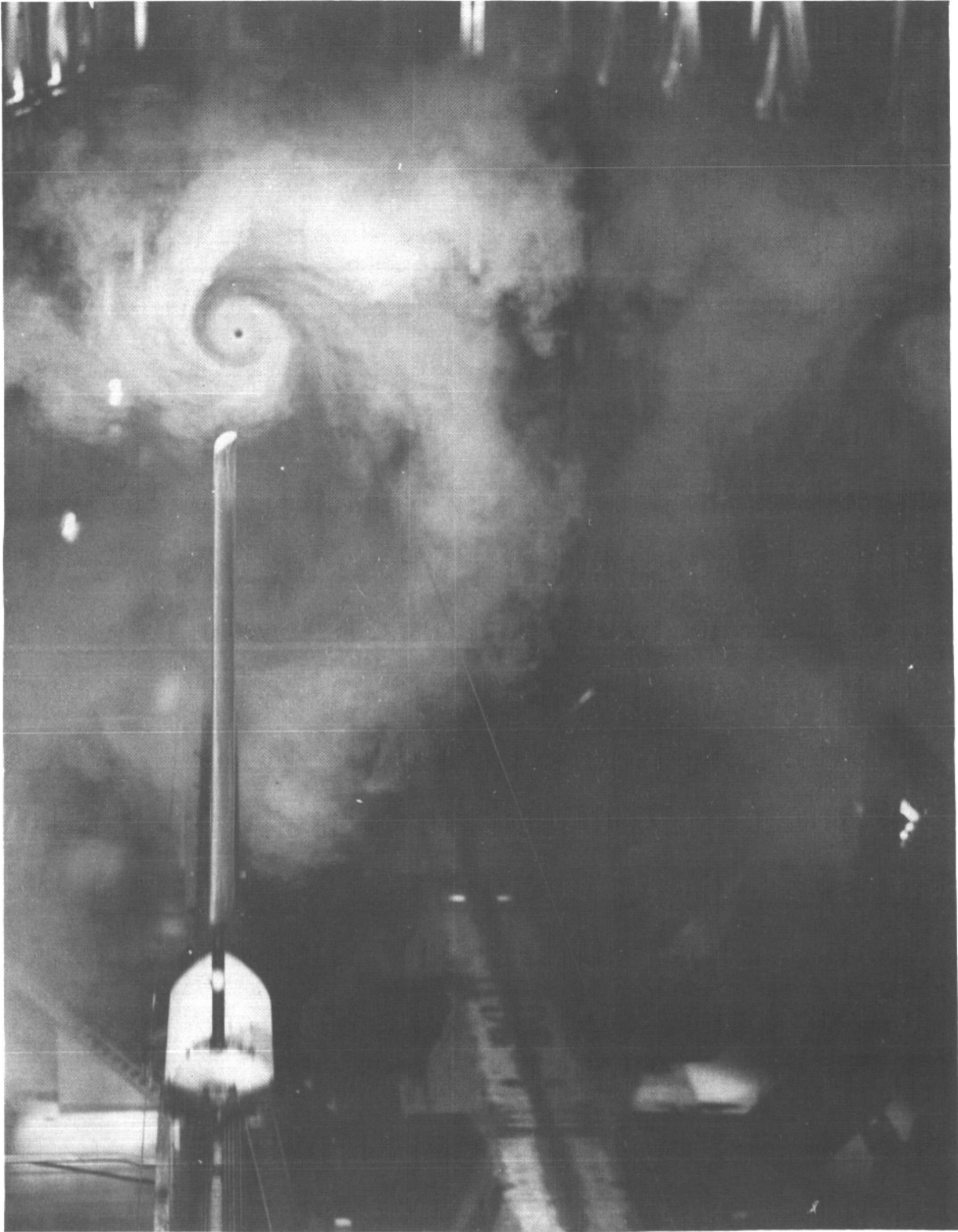


Figure 4. Drawing of vortex turbine blade planforms tested. All dimensions are in inches.



L-85-107
Figure 5. Smoke flow visualization of wingtip vortex created by an unswept untapered semispan lifting wing
in the Langley Vortex Research Facility.

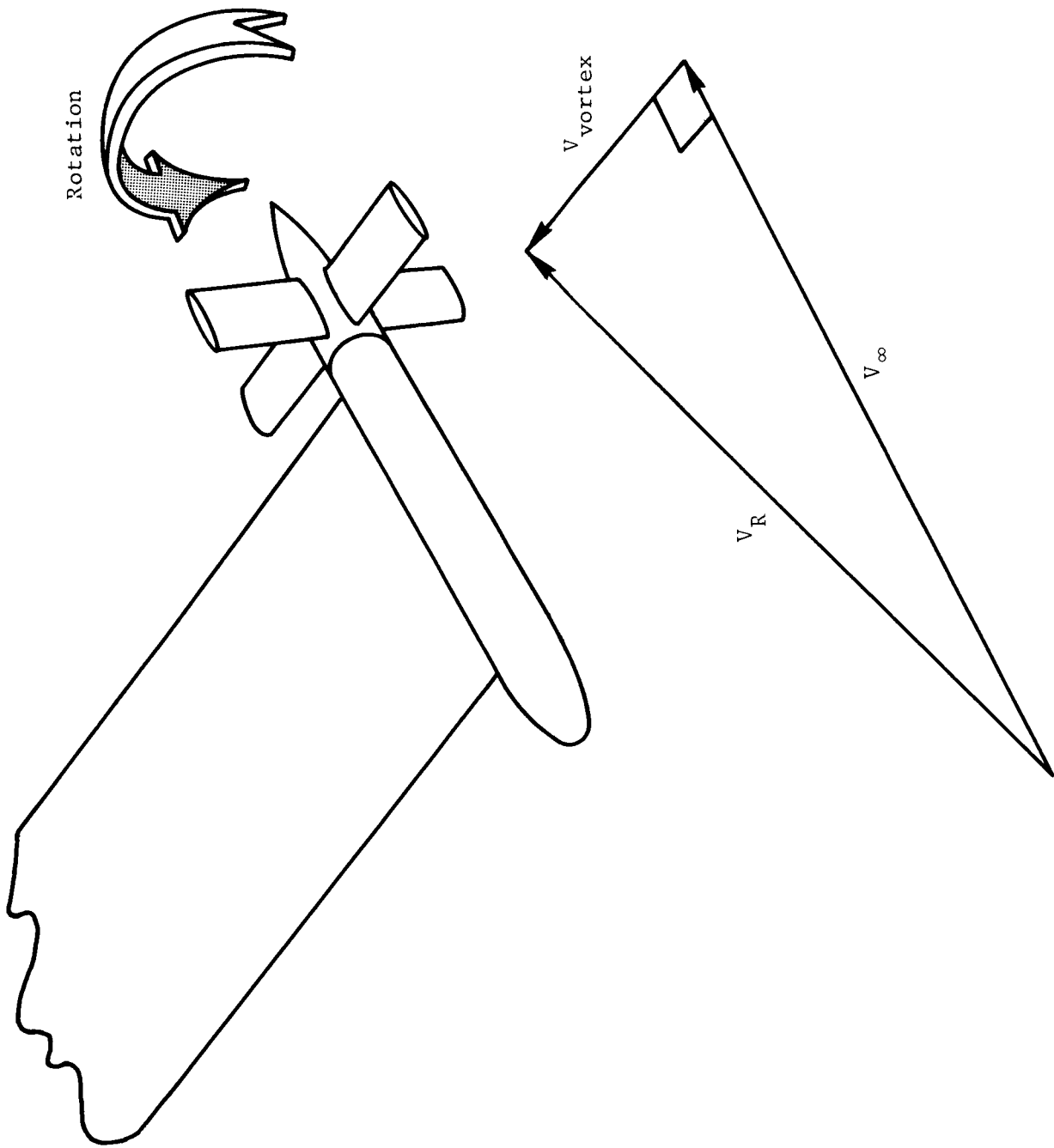


Figure 6. Sketch of vortex turbine with vectorial description of vortex and stream flows which produce the resultant velocity affecting the turbine blades.

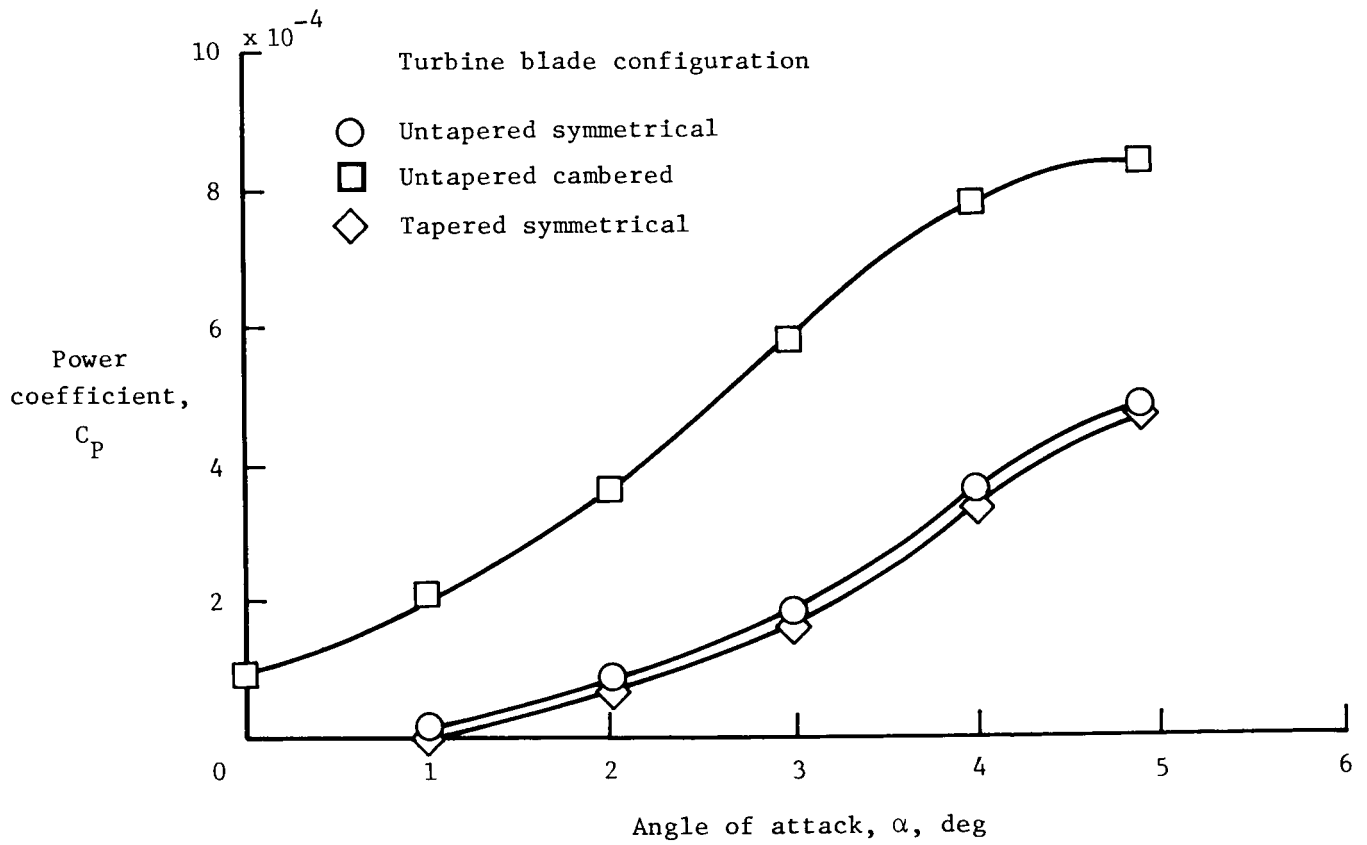
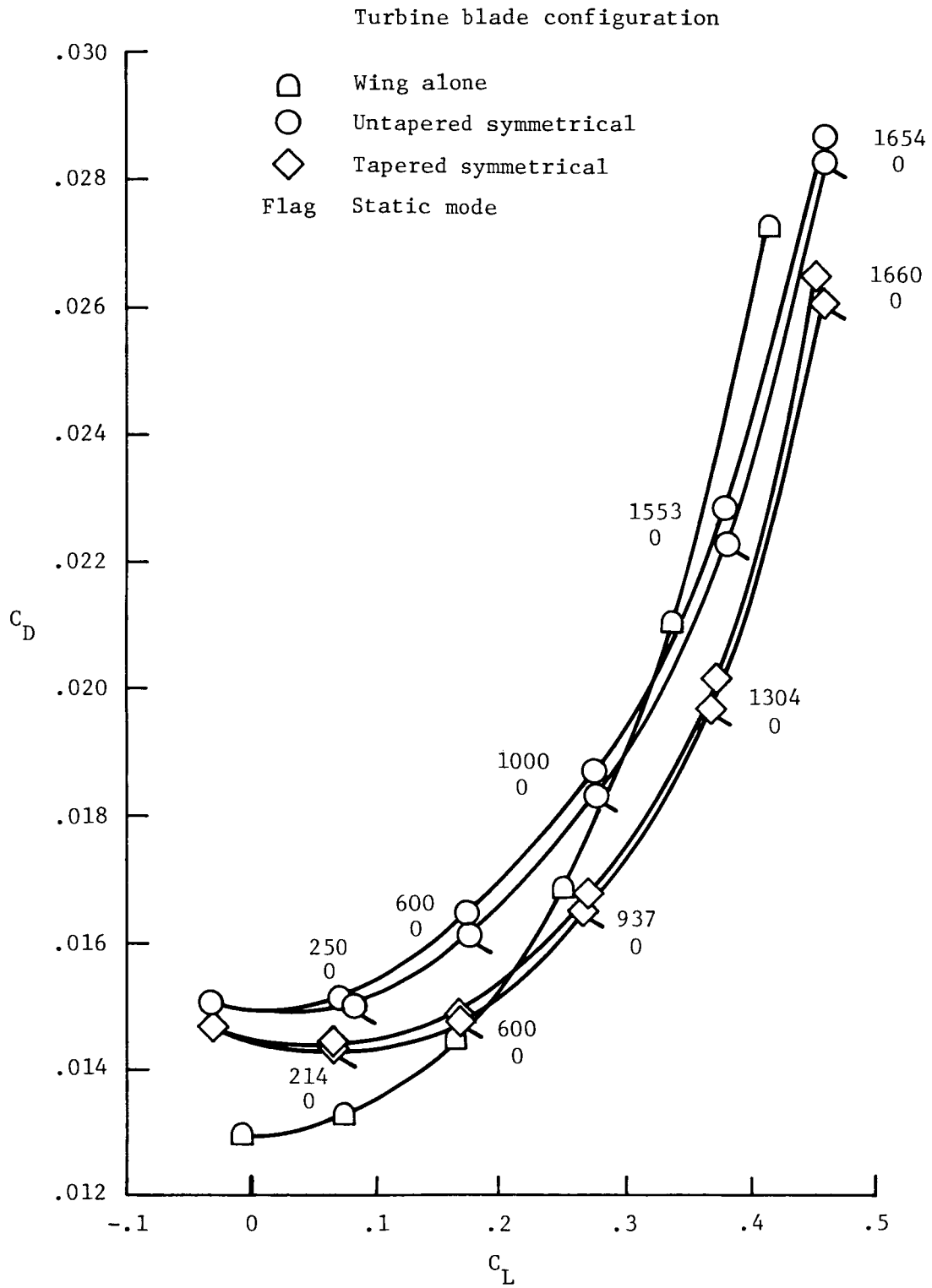
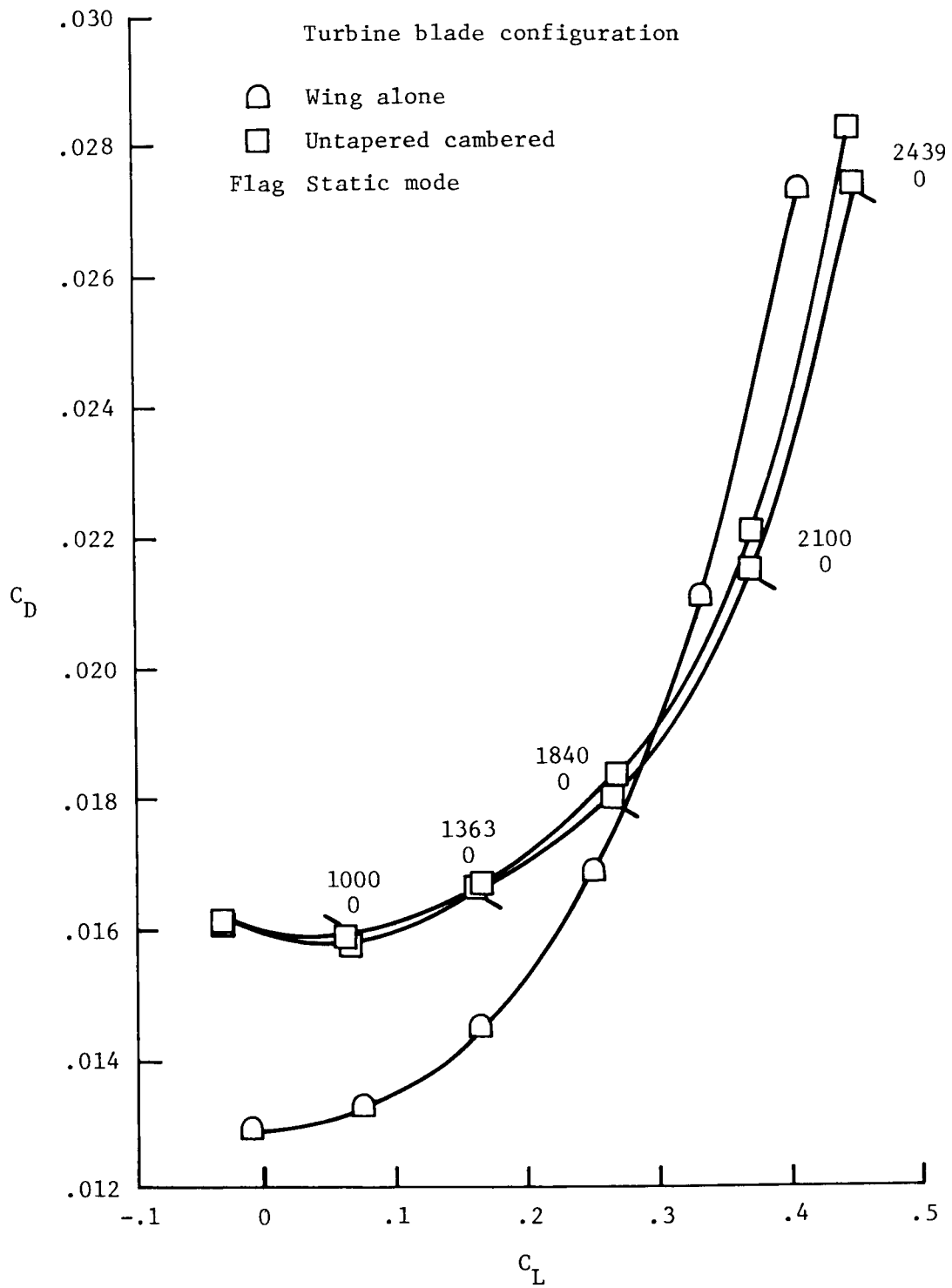


Figure 7. Power coefficient recovered from vortex turbine versus angle of attack for various vortex turbine blade designs. Turbine rotating.



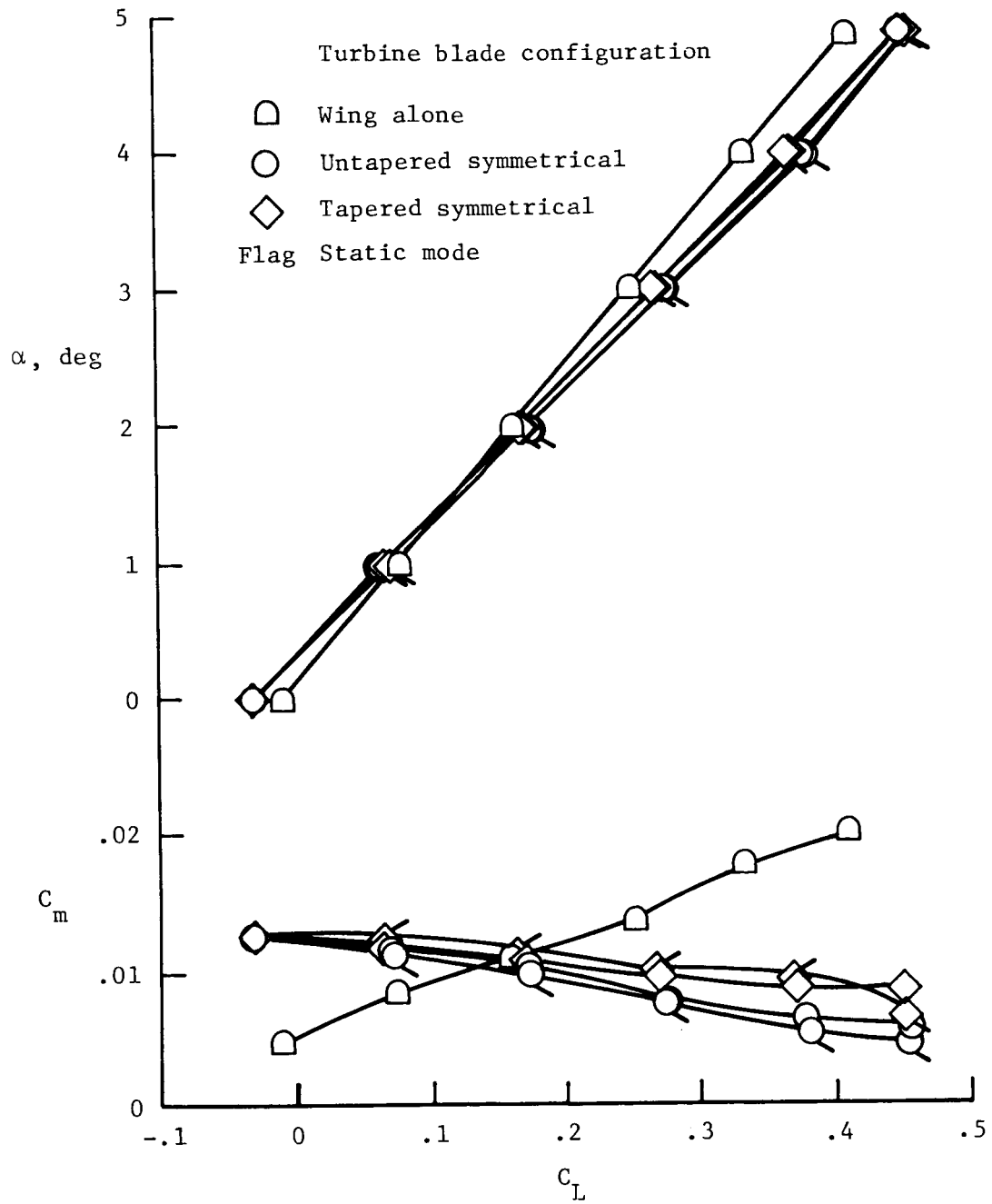
(a) Drag coefficient versus lift coefficient for wing alone and with untapered and tapered symmetrical turbine blades.

Figure 8. Basic aerodynamic characteristics of various turbine blade configurations. Numbers next to data points are blade rotational speeds in revolutions per minute.



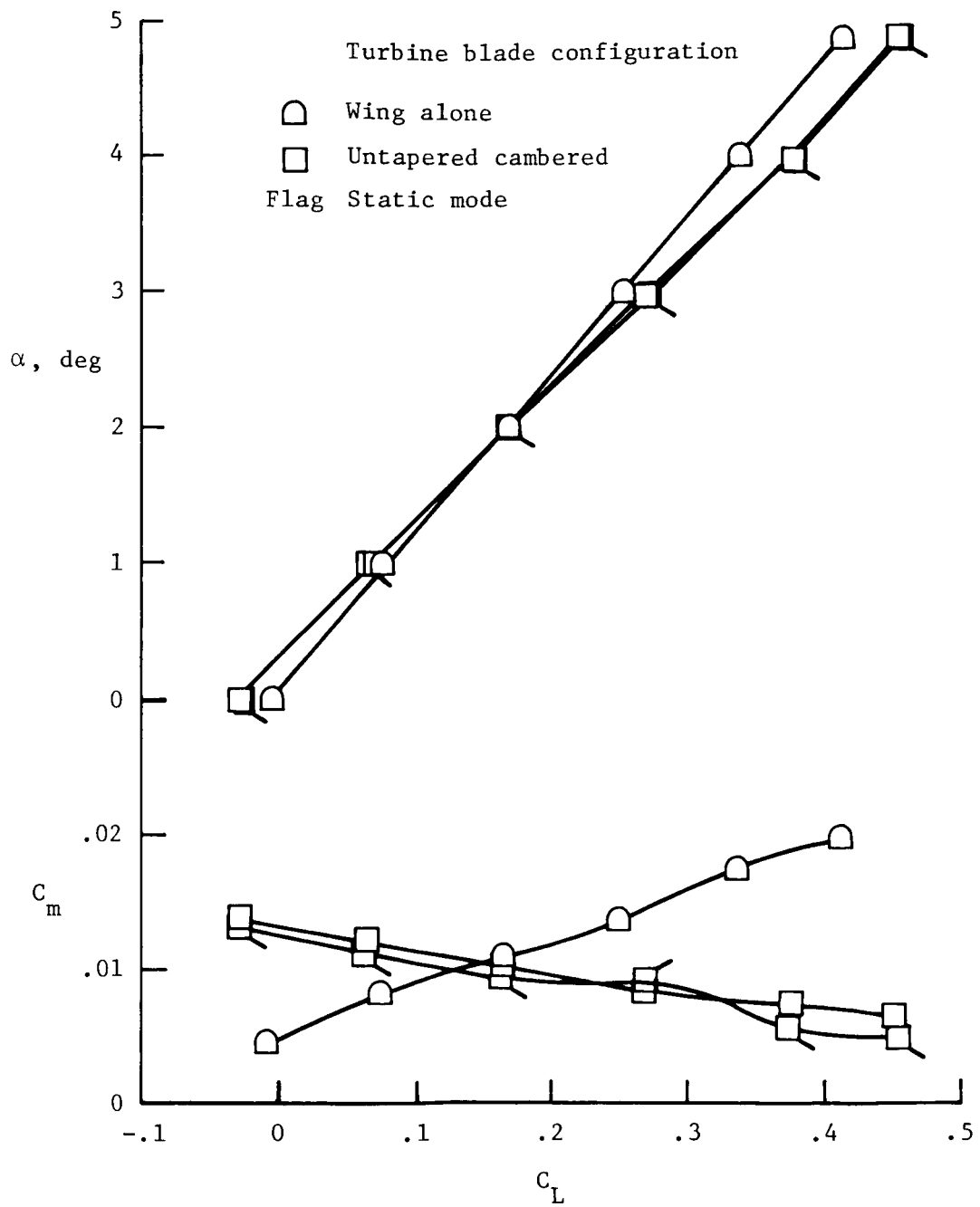
(b) Drag coefficient versus lift coefficient for wing alone and with untapered cambered turbine blades.

Figure 8. Concluded.



(a) Lift coefficient versus angle of attack and pitching-moment coefficient for wing alone and with untapered and tapered symmetrical turbine blades.

Figure 9. Basic aerodynamic characteristics with and without vortex turbine installed.



(b) Lift coefficient versus angle of attack and pitching-moment coefficient for wing alone and with untapered cambered turbine blades.

Figure 9. Concluded.

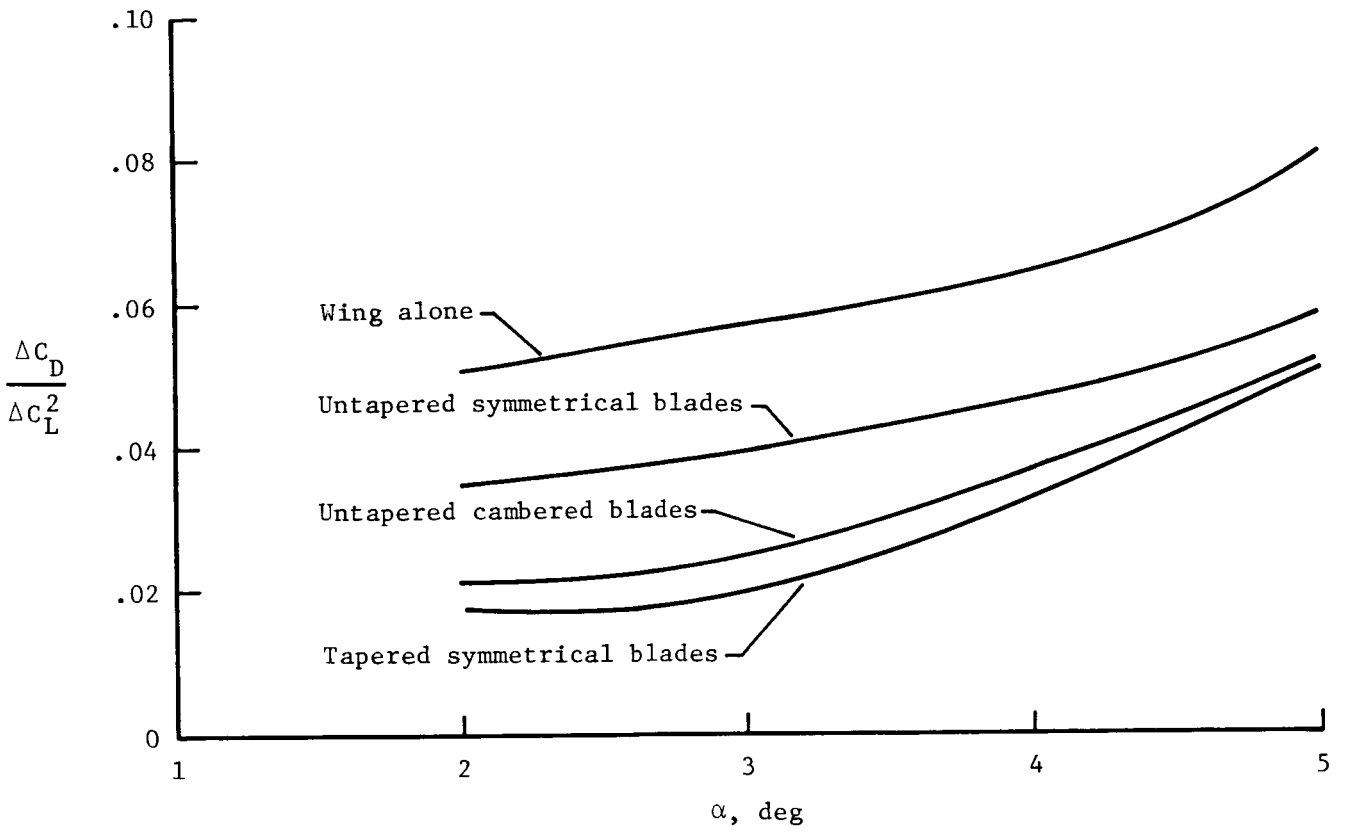


Figure 10. Drag-due-to-lift factor of wing with and without vortex turbine configurations installed. Turbine rotating.

1. Report No. NASA TP-2468		2. Government Accession No.		3. Recipient's Catalog No.	
4. Title and Subtitle Exploratory Wind-Tunnel Investigation of a Wingtip-Mounted Vortex Turbine for Vortex Energy Recovery				5. Report Date June 1985	
				6. Performing Organization Code 505-45-43-05	
7. Author(s) James C. Patterson, Jr., and Stuart G. Flechner				8. Performing Organization Report No. L-15795	
				10. Work Unit No.	
9. Performing Organization Name and Address NASA Langley Research Center Hampton, VA 23665				11. Contract or Grant No.	
				13. Type of Report and Period Covered Technical Paper	
12. Sponsoring Agency Name and Address National Aeronautics and Space Administration Washington, DC 20546				14. Sponsoring Agency Code	
				15. Supplementary Notes	
16. Abstract An exploratory investigation has been conducted at the Langley Research Center to determine the possibility of recovering, with a turbine-type device, part of the energy loss associated with the lift-induced vortex system. Tests were conducted on a semispan model with an unswept, untapered wing, with and without a wingtip-mounted vortex turbine. Three sets of turbine blades were tested to determine the effect of airfoil section shape and planform. The tests were conducted at a Mach number of 0.70 over an angle-of-attack range from 0° to 4° at a Reynolds number of 3.82×10^6 based on the wing reference chord of 13 in.					
17. Key Words (Suggested by Authors(s)) Vortex Vortex turbine Energy recovery Induced-drag reduction Vortex dissipation			18. Distribution Statement Unclassified—Unlimited Subject Category 02		
19. Security Classif.(of this report) Unclassified		20. Security Classif.(of this page) Unclassified		21. No. of Pages 22	22. Price A02

National Aeronautics and
Space Administration

Washington, D.C.
20546

Official Business

Penalty for Private Use, \$300

THIRD-CLASS BULK RATE

Postage and Fees Paid
National Aeronautics and
Space Administration
NASA-451



NASA

POSTMASTER: If Undeliverable (Section 158
Postal Manual) Do Not Return
